Layer Korringa-Kohn-Rostoker theory for close-spaced planes of atoms

J. M. MacLaren
Theoretical Division, MS-B262, Los Alamos National Laboratory, Los Alamos, New Mexico 87545

S. Crampin and D. D. Vvedensky
The Blackett Laboratory, Imperial College, London SW7 2BZ, United Kingdom
(Received 30 January 1989; revised manuscript received 6 July 1989)

Layer Korringa-Kohn-Rostoker (LKKR) approaches that calculate interlayer scattering using a plane-wave basis set cannot treat systems in which the interplanar spacing becomes small. This problem is most acute at band energies at which electronic lifetimes are long and the scattering strong. Taking a face-centered-cubic material as an example, solutions for the simplest of grain boundaries, the $\Sigma 5$ tilt, requires the stacking together of (210) planes. The planar spacing for this system is too small to allow the conventional LKKR methods to be applied. We estimate needing over 500 plane waves to converge the interlayer scattering in this case. We describe here a solution to layer coupling that allows for this situation. The technique optimizes the sizes of the angular momentum and plane-wave basis sets and thus provides an important extension to LKKR schemes. The ideas developed can be easily applied to both low-energy electron diffraction and photoemission.

I. INTRODUCTION

Techniques for calculating electronic and spectroscopic properties of surfaces and interfaces by first partitioning the system into layers of atoms and then using multiple-scattering theory are collectively referred to as layer Korringa-Kohn-Rostoker (LKKR) approaches.[1-6] These methods can correctly treat infinite systems, such as an isolated surface, without imposing three-dimensional translational symmetry. This is achieved by first solving for the scattering operators for each layer using an angular momentum basis set and a two-dimensional (2D) KRR theory.[7] Since each layer has 2D translational symmetry, then a 2D Fourier transform block diagonalizes the layer scattering matrices at each $\mathbf{k}$ in the 2D Brillouin zone (BZ). The scattering properties of each layer can also be described in terms of plane-wave scattering matrix elements, by considering the scattering of an incident plane wave at energy E and $\mathbf{k}$ by an isolated layer of atoms. This plane wave is then expanded into spherical waves about each atomic site in the layer and all intralayer multiple scattering summed within this basis. The resulting scattered partial waves can be transformed back into plane waves using a Huygen's construction. Individual layers can then be coupled together in the plane-wave basis in a recursive manner to build up the solid. For example, if the scattering matrices of the individual layers are identical, the reflectivity of a semi-infinite half-space can be found using layer doubling. This reflectivity would be the quantity needed to find the low-energy electron-diffraction (LEED) spectra of an ideal surface (for a more detailed discussion of the usual implementation of the LKKR method we refer the reader to the previous paper,[8] denoted as I).

These recursive algorithms involve the effective transmission matrix of the layer which includes a term involving no intralayer scattering (direct) in addition to corrections from multiple scattering in the layer. The direct term is represented by the 2D Bloch free-space Green's function at the given $\mathbf{k}$, which is diagonal in the plane-wave basis. Thus the only internal angular momentum summations which can cause convergence problems also involve the product of an atomic t matrix which limits the contribution from high angular momentum channels.

The difficulties associated with the close-spaced layers can easily be seen by examining the form of the plane-wave basis functions which couple the layers. The basis functions coupling two layers separated by the vector $\mathbf{c}=(\mathbf{c}_{\parallel},c_z)$ converge uniformly provided the z component of the interlayer spacing is nonzero, since for large 2D reciprocal lattice vectors ($\mathbf{g}$) they take the form [see Eqs. (22) and (23) of I]

$$\langle \mathbf{r}|\mathbf{K}_{\mathbf{g}}^{\pm}\rangle|_{\mathbf{r}=\mathbf{c}}=\exp[i(\mathbf{k}+\mathbf{g})\cdot c_{\parallel}+i\sqrt{2E-(\mathbf{k}+\mathbf{g})^2}|c_z|] \rightarrow e^{i(\mathbf{k}+\mathbf{g})\cdot\mathbf{c}_{\parallel}}e^{-g|c_z|} \quad \text{as } g\rightarrow\infty\ , \tag{1}$$

where $\mathbf{k}$ is the 2D momentum. Thus, while exponentially convergent, the rate clearly depends on the size of c_z. In systems where c_z is small, many vectors are required to converge the interlayer scattering to a prescribed accuracy. Two further factors work against this basis for close-spaced layers. First, the number of 2D reciprocal lattice vectors at a given $\mathbf{g}$ grows like g thus exacerbating rates of convergence. Second, for any given system, stacking higher Miller index planes together results not only in the layers becoming closer together but also in increasing the size of the 2D layer unit and hence decreasing the magnitude of the g vectors. These two factors conspire to make many interesting systems (e.g., grain boundaries and stepped surfaces) computationally intractable with the usual LKKR methods.

We have found that the dimensionless quantity $g_{\min}c_z$ monitors whether the system can or cannot be reasonably calculated with the simpler LKKR method, where $g_{\min}$ is the smallest reciprocal lattice vector. If this number is larger than 5, then coupling all the layers in a plane-wave basis is feasible, as discussed previously. If not, then it is more efficient to implement the formalism which we discuss in this paper. The problem becomes more acute at band energies arising in photoemission calculations[9] or in electronic structure calculations,[4–6] where one encounters long electron lifetimes (often infinite) and strong multiple scattering. At these energies only a few partial waves (say up to $l=2$ for transition metals) are required, but many plane waves. For a face-centered-cubic (fcc) first-row transition metal, we have found that in order to converge the density of states (DOS) to four significant figures, over 30 plane waves were required compared to nine ($l=2$) partial waves. This calculation was done along a favorable crystal direction, i.e., stacking (100) planes together which have the second largest interplanar separation, and the second smallest 2D layer unit cell for the fcc structure. Thus, at band energies, *most* systems of interest fall into the category where the plane-wave basis set is bigger and often too big to be practical in calculations. It is the purpose of this paper to report an algorithm for solving this problem. The solution, at the expense of some algebraic complexity, provides a method of optimizing both basis sets.

This work is motivated by a study of the electronic properties of a $\Sigma 5$ tilt grain boundary, which is one of the simplest possible grain boundaries. This occurs when the stacking sequence along the (210) direction and its mirror image join, the crystallographic mismatch forming the grain boundary (see Fig. 1). There has been considerable interest in this model grain boundary since grain boundaries in general and similar defects in crystals are important in understanding the mechanical properties of metals and alloys. In particular, their influence upon the fracture behavior of intermetallics has been the thrust of considerable experimental and theoretical work.[10,11] Our goal, therefore, is to provide accurate first-principles calculations for this system and to provide a technique capable of treating complex grain boundaries both with and without segregated impurities. Layer coupling of (210) planes in a plane-wave basis set was found to not converge due to the small interplanar spacing ($g_{\min}c_z \simeq 1$). The problems associated with close-spaced layers has also been noticed by other groups[12] as a major impediment to LKKR-type calculations. Solutions to this problem, such as the combined-space method,[13] can only treat a finite number of close-spaced layers. In the case of the $\Sigma 5$ tilt grain boundary this method is totally inappropriate since there are an infinite number of close-spaced layers forming the bulk. Thus the range of problems which can be handled within the LKKR framework is increased substantially with our method.

The aim of this paper is to find an expression for the Green's function for an atom embedded in a layered solid using multiple-scattering theory. The outline of the paper is as follows. In Sec. II we give the elements of LKKR theory necessary for a discussion of closely

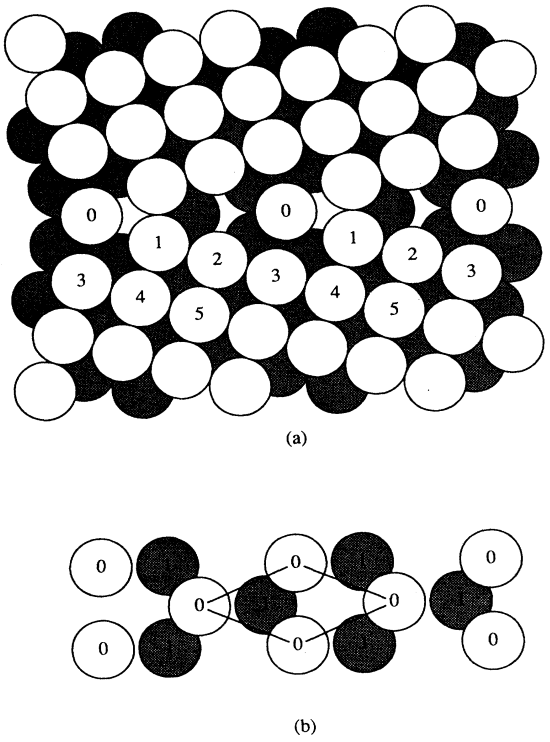

FIG. 1. (a) The atomic arrangement of the $\Sigma 5$ grain boundary used in the calculations. The atomic planes are stacked along the [210] direction; (b) plan view of 2D unit layer unit cell showing atoms at the boundary (open circles) and those below, from plane 1 (shaded circles).

spaced layers. Most of the formalism is given in I, the preceding paper so we will just refer to the relevant equations. In Sec. III we will show how to add a layer onto a stack of layers in such a manner that convergence can always be achieved no matter how close together the interplanar spacing is. In principle the bulk half-space scattering matrices can be built up this way, though it is faster to use a layer-doubling technique. In order to perform calculations in reasonable computing times we found it necessary to adopt a layer-doubling technique. One suitable for close-spaced layers is discussed in Sec. IV. Once the bulk matrices have been found, then any layers which are different from the bulk need to be added on one at a time using the ideas presented in Sec. III. In a self-consistent interface calculation, for example, only the potentials of layers at and close to the interface are allowed to relax. The more distant layers are fixed with bulk potentials. Thus, the relaxed layers are now different from the bulk. Scattering matrices for all the layers to the left and to the right of a particular layer along with this layer's scattering matrix are all that is required to calculate the Green's function about atoms in this particular layer using equations given in Sec. II. In Sec. V we illustrate the convergence properties of the method with self-consistent calculations on a $\Sigma 5$ tilt boundary in nickel. The technique can, of course, be used to advantage in both photoemission and LEED calculations for systems with small interplanar spacings.

II. THEORY

The site-diagonal single-particle Green's function from which the electronic properties of the layered system can be found is given Eq. (32) of I. To make this paper easier to follow we reproduce here

$$G(\mathbf{r},\mathbf{r}')=-4i\kappa\sum_{L}\tilde{R}_{L}^{\alpha_i}(\mathbf{r}_<)R_{L}^{(1)\alpha_i}(\mathbf{r}_>)-\frac{4i\kappa}{\Omega}\sum_{LL'}R_{L}^{\alpha_i}(\mathbf{r}')(t_l^{\alpha_i})^{-1}\left[\int_{\Omega}d\mathbf{k}\,\tau_{iLL'}^{\alpha\alpha}(\mathbf{k})-\delta_{LL'}t_{l'}^{\alpha_i}\right](t_{l'}^{\alpha_i})^{-1}\tilde{R}_{L'}^{\alpha_i}(\mathbf{r}) , \tag{2}$$

where $\kappa=\sqrt{2E}$, $r_{>(<)}$ is the greater (lesser) of r and r', $R_L^{\alpha_i}(\mathbf{r}_>)$ and $R_L^{(1)\alpha_i}(\mathbf{r}_>)$ are the regular and irregular solutions to the isolated muffin tin, formed from products of spherical harmonics and solutions to the radial Schrödinger equation. The tilde signifies that only the spherical harmonic is complex conjugated. The scattering-path operator of a particular layer, in the LKKR formalism of I, was found in terms of an effective reflectivity of the solid excluding this layer [Eq. (18) of I]. The solutions to the equations of motion for the scattering-path operators [Eq. (13) of I] can also be written in the following form:

$$\begin{aligned}\tau_i=&\{1+[T_r^{i+1}+(1+T_r^{i+1}\mathcal{G})(1-T_l^{i-1}\mathcal{G}T_r^{i+1}\mathcal{G})^{-1}T_l^{i-1}(1+\mathcal{G}T_r^{i+1})]\mathcal{G}\}T_i\\&\times\{1-\mathcal{G}[T_r^{i+1}+(1+T_r^{i+1}\mathcal{G})(1-T_l^{i-1}\mathcal{G}T_r^{i+1})^{-1}T_l^{i-1}(1+\mathcal{G}T_r^{i+1})]\mathcal{G}T_i\}^{-1} .\end{aligned} \tag{3}$$

In terms of τ_i, τ_l is given by

$$\tau_l=(1+\tau_i\mathcal{G})(1+T_r^{i+1}\mathcal{G})T_l^{i-1}(1-\mathcal{G}T_r^{i+1}\mathcal{G}T_l^{i-1})^{-1} \tag{4}$$

and τ_r by

$$\tau_r=(1+\tau_i\mathcal{G})(1+T_l^{i-1}\mathcal{G})T_r^{i+1}(1-\mathcal{G}T_l^{i-1}\mathcal{G}T_r^{i+1})^{-1} , \tag{5}$$

and it is this form that we use in solving the case when the layers are close spaced. Equation (3) will form the basis of our solution to the closely spaced layer Green's function since the matrix elements of τ_i are found directly from it. However in treating the generalized layer-doubling equations we will need Eqs. (4) and (5) as well, since we need the full T matrix of a three-body system, which is found from the sum of the three individual τ operators.

In our solution, we couple the three scattering operators T_l, T_r, and T_i in such a way that all scattering paths between *adjacent* layers are calculated in an angular momentum basis, while all the other scattering paths are summed with the plane wave basis set. For complete generality each of these scatterers may be several layers grouped together (i.e., a noncoplanar layer) so that the shortest direct plane-wave scattering path may be made arbitrarily long (in real space), and certainly such as to ensure that $g_{\min}c_z>5$. Hence, convergence can always be achieved by a suitable partitioning of atoms into layers. In our example of (210) planes each layer was made of two planes, thus the shortest plane-wave displacement is four times the (210) interplanar spacing. This differs from the usual LKKR approaches where all planes are coupled in the plane-wave basis set and that of Gonis,[14,15] where the *all* planes would be coupled in the angular momentum basis set.

III. STACKING LAYERS TOGETHER

In this section we outline the procedure for calculating the half-space reflectivities T_l and T_r which enter Eq. (3). We consider explicitly the right half-space and similar arguments hold for the left-half space. Formally the result of adding a layer onto a stack of layers can be written as

$$\begin{aligned}T_r^{i-1}=&T_{i-1}+(1+T_{i-1}\mathcal{G})T_r^i(1-\mathcal{G}T_{i-1}\mathcal{G}T_r^i)^{-1}\\&\times(1+\mathcal{G}T_{i-1}) .\end{aligned} \tag{6}$$

We ensure, for the reasons discussed, that products like $T_{i-1}\mathcal{G}T_r^i$ have internal summations in the angular momentum basis since these are adjacent scatterers. Thus there are four possible hybrid matrix elements for the scattering from the stack of layers, namely all four possible combinations of plane and spherical wave couplings. For example, on adding a layer to the stack, a scattering path involving the scattering first from the layer and then from the stack would involve internal summations in the angular momentum basis since these are adjacent scattering events. On the other hand, the direct term which would pass through the added layer and involve only scattering from the stack would be represented by a plane-wave term. This leads to four coupled equations for the hybrid matrices of T_r. These matrix elements are labelled:

$$\begin{aligned}R_{ri}^{gg}&=\langle\mathbf{K}_{\mathbf{g}}^{-}|\mathcal{G}T_r^i\mathcal{G}|\mathbf{K}_{\mathbf{g}'}^{+}\rangle ,\\R_{ri}^{gL}&=\langle\mathbf{K}_{\mathbf{g}}^{-}|\mathcal{G}T_r^i\mathcal{G}|L'\beta_{i-1}\rangle ,\\R_{ri}^{Lg}&=\langle L\alpha_{i-1}|\mathcal{G}T_r^i\mathcal{G}|\mathbf{K}_{\mathbf{g}'}^{+}\rangle ,\\R_{ri}^{LL}&=\langle L\alpha_{i-1}|\mathcal{G}T_r^i\mathcal{G}|L'\beta_{i-1}\rangle ,\end{aligned} \tag{7}$$

where the origin of the matrices is placed at the next leftmost layer for convenience and the superscripts denote the *basis type* and *not* individual matrix elements. In order to find the matrix representation necessary for calculations of the four coupled equations we first expand the second term in (6) into four terms. The four hybrid matrix elements, as expressed by (7), are found from this expanded version of (6). After some algebra we arrive at

$$\begin{aligned}R_{ri-1}^{gg}=&P_i^{+}R_{ri}^{gg}P_i^{-}\\&+P_i^{+}(R_{ri}^{gL}+\Gamma_{i-1}^{+gL})(1-T_{i-1}^{LL}R_{ri}^{LL})^{-1}T_{i-1}^{LL}\\&\times(R_{ri}^{Lg}+\Gamma_{i-1}^{-Lg})P_i^{-} ,\end{aligned} \tag{8a}$$

$$R_{ri-1}^{gL}=P_i^+R_{ri}^{gg}P_i^-\Gamma_{i-1}^{-gL}+P_i^+(R_{ri}^{gL}+\Gamma_{i-1}^{+gL})(1-T_{i-1}^{LL}R_{ri}^{LL})^{-1}T_{i-1}^{LL}\times(R_{ri}^{Lg}P_i^-\Gamma_{i-1}^{-gL}+G_i^-)\ , \tag{8b}$$

$$R_{ri-1}^{Lg}=\Gamma_{i-1}^{+Lg}P_i^+R_{ri}^{gg}P_i^-+(\Gamma_{i-1}^{+Lg}P_i^+R_{ri}^{gL}+G_i^+)(1-T_{i-1}^{LL}R_{ri}^{LL})^{-1}\times T_{i-1}^{LL}(R_{ri}^{Lg}+\Gamma_i^{-Lg})P_i^-\ , \tag{8c}$$

$$R_{ri-1}^{LL}=\Gamma_{i-1}^{+Lg}P_i^+R_{ri}^{gg}P_i^-\Gamma_{i-1}^{-gL}+(\Gamma_{i-1}^{+Lg}P_i^+R_{ri}^{gL}+G_i^+)(1-T_{i-1}^{LL}R_{ri}^{LL})^{-1}\times T_{i-1}^{LL}(R_{ri}^{Lg}P_i^-\Gamma_{i-1}^{-gL}+G_i^-)\ , \tag{8d}$$

where the overlap between the two bases Γ needed for transformation between plane and spherical waves is given by Eq. (25) of I. $G_i^{\pm}$ are the spherical wave representations of the 2D Bloch free-space Green's function $\mathcal{G}$, given by

$$G_i^+=\langle L\alpha_i|\mathcal{G}|L'\beta_{i+1}\rangle\ ,\qquad G_i^-=\langle L\beta_{i+1}|\mathcal{G}|L'\alpha_i\rangle\ . \tag{9}$$

Formulas suitable for the calculation of the matrix elements in (9) are complex and have been given by Kambe,[16] so we will not reproduce the results here but refer the reader to these papers. In (8) the plane wave expansions of the 2D Bloch free-space Green's function P are given by Eq. (26) of I, and the individual layer scattering matrices, T_i, by Eq. (21) of I.

In contrast the usual LKKR method yields only one equation as a solution to (6), which is expressed solely in plane waves; this is

$$R_{ri-1}^{gg}=P_i^+T_{i-1}^{+-}P_i^-+P_i^+(1+T_{i-1}^{++})R_{ri}^{gg}(1-T_{i-1}^{-+}R_{ri}^{gg})^{-1}\times(1+T_{i-1}^{--})P_i^-\ . \tag{10}$$

The matrices $T_i^{\pm\pm}$ are the plane-wave scattering matrix elements of layer i where the $\pm$ superscripts label the direction of incident and scattered plane waves [Eq. (24) of I].

In principle, Eqs. (8a)–(8d) can be iterated to find the bulk scattering matrices by adding one layer at a time or by regarding these as a self-consistent relation. These nonlinear equations can be solved by standard techniques. One such approach is by taking the result of one pass and mixing it with the input to use as input to the next cycle. Acceleration of this scheme, resulting in significant computational savings, can be obtained by developing a generalized layer-doubling method, which we shall do in the next section. The scattering matrices for the left half-space follow in an analogous manner. Once all the hybrid matrix elements for the left and right half-spaces have been found they are used in conjunction with Eq. (3) to give the appropriate matrix elements of τ_i necessary for the Green's-function calculation. Again taking care to separate out the adjacent scattering events τ_i can be expressed in the following form:

$$\langle L\alpha_i|\tau_i|L'\alpha_i\rangle=(1+\Delta_i^{LL})T_i^{LL}(1-\Delta_i^{LL}T_i^{LL})^{-1}\ . \tag{11}$$

After some manipulation Δ_i^{LL} is given by

$$\Delta_i^{LL}=T_{ri+1}^{LL}+T_{ri+1}^{LL}+(T_{ri+1}^{Lg}+T_{li-1}^{Lg}T_{ri+1}^{gg})(1-T_{li-1}^{gg}T_{ri+1}^{gg})^{-1}T_{li-1}^{gL}+(T_{li-1}^{Lg}+T_{ri+1}^{Lg}T_{li-1}^{gg})(1-T_{ri+1}^{gg}T_{li-1}^{gg})^{-1}T_{ri+1}^{gL}\ , \tag{12}$$

whereas in the usual LKKR method the half-space reflectivities are determined solely in the plane-wave basis set. The hybrid matrix elements needed in Eq. (12) are

$$T_{ri+1}^{LL}=\Gamma_i^{+Lg}T_{ri+1}^{gg}\Gamma_i^{-gL},\quad T_{li-1}^{LL}=\Gamma_i^{-Lg}T_{li-1}^{gg}\Gamma_i^{+gL}\ ,$$
$$T_{ri+1}^{Lg}=\Gamma_i^{+Lg}T_{ri+1}^{gg},\quad T_{li-1}^{Lg}=\Gamma_i^{-Lg}T_{li-1}^{gg}\ , \tag{13}$$
$$T_{ri+1}^{gL}=T_{ri+1}^{gg}\Gamma_i^{-gL},\quad T_{li-1}^{gL}=T_{li-1}^{gg}\Gamma_i^{+gL}\ .$$

Again the superscript denotes basis type rather than an individual matrix element.

Equation (6) could be solved soley in terms of the angular momentum basis set. This is the approach suggested by Gonis[14] and implemented by Zhang and Gonis.[15] However, the direct terms in the angular momentum basis involve nondiagonal Green's functions. Upon iteration products of Green's functions involve internal summations which are not controlled by atomic t matrices and can show slow convergence in certain geometries, thus necessitating larger matrices. In our algorithm, we have taken great care to ensure that all the internal summations are controlled by keeping the direct terms in a plane-wave basis set. We have achieved this by solving the more complicated three-center scattering problem so that adjacent scattering can be treated explicitly.

IV. GENERALIZED LAYER-DOUBLING EQUATIONS

While (8a)–(8d) can be used to calculate reflectivities as outlined at the end of Sec. III, the more conventional technique of layer doubling may also be formulated in the current framework. The aim of layer doubling[17] is to accelerate the construction of the half-space matrices and reduce the computing time needed. The conventional layer-doubling equations (see paper I), which result from the two-center scattering problem cannot be used in the present situation, since there is no way to isolate the adjacent scattering separately from other scattering paths. The way around this is to combine three scatterers at once, using the three-center scattering formulas (3)–(5) to form the total T matrix of such a system ($T=\tau_l+\tau_i+\tau_r$). The left and right scatterers are the result of a previous "double" and the central scatterer T_i is the basic layer repeat unit for the bulk. Thus after n "doubles" the stack contains $2^{n+1}-1$ layers as against 2^n for the conventional method. As in standard layer doubling we have four basic equations for T^{++}, T^{+-}, T^{-+}, and T^{--} which describe transmission and reflection from either side of the stack of layers. These combine to double the stack as,

$$T^{++}=\tau_i+(T_l^{++}+T_r^{+-})\tau_i+T_l^{++}(1-T_r^{+-}T_l^{-+})^{-1}[1+T_r^{++}+(T_r^{+-}T_l^{-+}+T_r^{+-})\tau_i]$$
$$+(1-T_r^{+-}T_1^{-+})^{-1}[T_r^{++}+T_r^{+-}T_l^{-+}+T_r^{+-}(T_l^{-+}T_r^{+-}+T_l^{-+})\tau_i]\,, \tag{14}$$

$$T^{+-}=\tau_i+T_l^{+-}+(T_l^{++}+T_r^{+-})\tau_i+T_1^{++}(1-T_r^{+-}T_l^{-+})^{-1}[T_r^{+-}T_l^{--}+T_l^{+-}+(T_r^{+-}T_l^{-+}+T_r^{+-})\tau_i]$$
$$+T_r^{+-}(1-T_l^{-+}T_r^{+-})^{-1}[1+T_l^{--}+(T_l^{-+}T_r^{+-}+T_l^{-+})\tau_i]\,, \tag{15}$$

$$T^{-+}=\tau_i+T_r^{-+}+(T_r^{--}+T_r^{-+})\tau_i+T_r^{--}(1-T_l^{-+}T_r^{+-})^{-1}[T_l^{-+}T_r^{++}+T_r^{-+}+(T_l^{-+}T_r^{+-}+T_l^{-+})\tau_i]$$
$$+T_l^{-+}(1-T_r^{+-}T_l^{-+})^{-1}[1+T_r^{++}+(T_r^{+-}T_l^{-+}+T_r^{+-})\tau_i]\,, \tag{16}$$

$$T^{--}=\tau_i+(T_l^{-+}+T_r^{--})\tau_i+(1-T_l^{-+}T_r^{+-})^{-1}[T_l^{--}+T_l^{-+}T_r^{+-}+T_l^{-+}(T_r^{+-}T_l^{-+}+T_r^{+-})\tau_i]$$
$$+T_r^{--}(1-T_l^{-+}T_r^{+-})^{-1}[1+T_l^{--}+(T_l^{-+}T_r^{+-}+T_l^{-+})\tau_i]\,, \tag{17}$$

where τ_i was given in (3). In the iteration of these equations we must remember to treat adjacent scatterings in spherical waves and the rest in plane waves. This results in 16 coupled equations due to all four possible couplings between plane and spherical waves for each of the above four equations. The details are straightforward but involve lengthy algebra since we now have 16 coupled matrix equations, and so will not be written down here. However the philosophy is identical to that given in Sec. III.

V. APPLICATION TO AN Σ5 TILT GRAIN BOUNDARY IN NICKEL

The method described above has been applied to an Σ5 tilt grain boundary in nickel, with the geometry as shown in Fig. 1. The structure was formed by reflecting semi-infinite stacks of (210) planes of fcc Ni followed by a relaxation of atoms in the layer labelled 1 to avoid overlap of the muffin-tin spheres, and a relaxation of atoms in the layer labelled 0 to maximize the number of nearest neighbors. To lowest order, this procedure yields the grain boundary structure obtained by embedded-atom methods.[11] The potentials of atoms in layers labelled $0,\ldots,5$ were allowed to relax during iteration to self-consistency, with potentials of more distant planes of atoms taken to be that of bulk nickel.

The bulk scattering matrices were converged using the generalized layer-doubling algorithm, typically within six or seven passes. The relaxed layers (atoms 0 to 5) were added subsequently by layer stacking. Convergence in the muffin-tin density of states (MTDOS) was achieved with 15 plane waves. This rate of convergence for a bulk nickel crystal along the [210] direction at a single **k** point in the Brillouin zone at a complex energy ($E_r=0.2$ hartree and $E_{\rm im}=0.005$ hartree) is shown in Fig. 2(a) and is contrasted with the behavior of the conventional LKKR method. The solid line shows the rapid convergence of the MTDOS calculated with the new code, while the old code (dotted line) clearly shows no convergence in this geometry. The central processor unit (CPU) time on a VAX 3000 workstation for these tests is shown in Fig. 2(b). The new code takes significantly longer at a fixed number of plane waves; however, it is roughly comparable at 15 plane waves to the old code with 30 plane waves. This time increase is predominantly due to the more complex layer-doubling algorithm. The details of the self-consistent algorithm involving energy and **k** in-

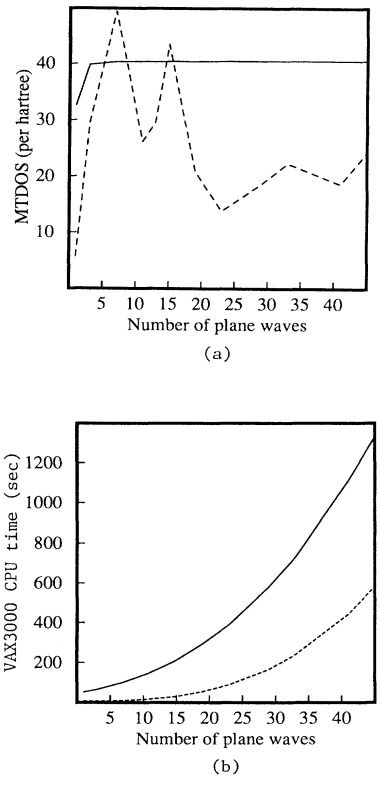

FIG. 2. (a) Convergence of MTDOS, evaluated at a single **k** point and at a complex energy of (0.2,0.005) hartree in the *d* bands, for bulk Ni made from an infinite stack of (210) planes as a function of the number of plane waves used in the interlayer scattering. The solid curve shows the results from the new code, compared to the dashed line of the normal LKKR calculation. (b) Comparison of the CPU time used by both codes. Timings for the new close-spaced code are shown by the solid line, and the usual LKKR code by the dashed line.

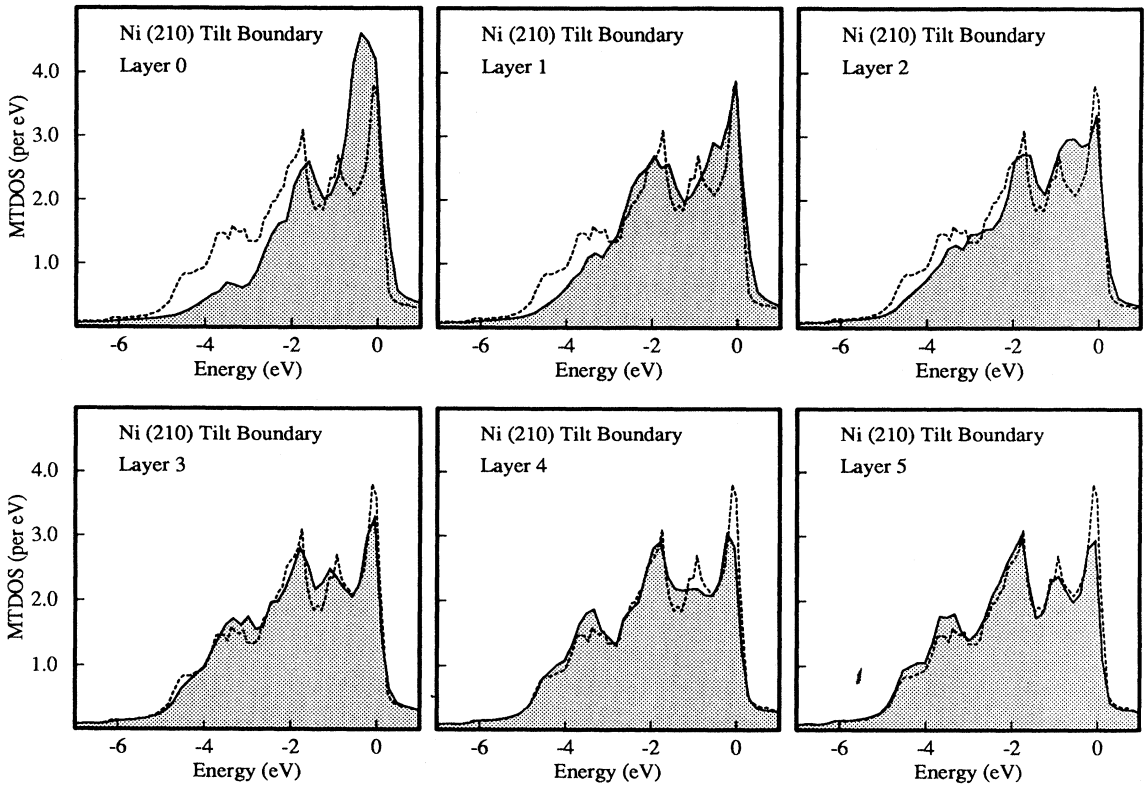

FIG. 3. MTDOS for atoms in the vicinity of a Σ5 tilt grain boundary in Ni (shaded curve), with the atom labelling is as in Fig. 1, contrasted to that of bulk Ni (dashed line). The Fermi energy is the zero of energy.

tegrations and the solution to Poisson's equation for the interface are described in I.

The MTDOS for atoms in the vicinity of an isolated Σ5 nickel tilt grain boundary are shown in Fig. 3. The changes are most pronounced on the interface layer, as would be expected since the perturbations from bulk geometry (in terms of coordination, bond length, and bond angle) are the greatest here. Most noticeable is the decrease in band width, resulting from the decrease in coordination. Full bulk fcc coordination is only achieved on the fifth atom from the boundary, and it is only on this layer that the full band width is recovered, with the MTDOS profile on the fifth atom appearing very similar to that of bulk nickel.[18] We notice that even at the boundary layer most of the main bulk MTDOS peaks appear to be present though shifted in energy. This occurs despite these nickel atoms only having four nearest (touching) neighbors. However second- and third-nearest neighbors are closer than in the bulk fcc crystal and consequently do interact with the boundary layer atoms. The large peak at the Fermi energy moves to lower energy, and this may well have consequences for the magnetization at the boundary. At present we are performing calculations on several metallic boundaries, and in the case of Ni a spin-polarized calculation, and the effects of segregated impurities. Preliminary reports of this work have appeared elsewhere.[19]

VI. CONCLUSIONS

The range of layered systems, for which LKKR schemes provide an elegant solution to the electronic structure, is greatly extended by the ability to treat close-spaced layers. To this end we have developed algorithms which can treat such systems and so remove the obstacle which has traditionally hindered LKKR methods. The solution is more complex and consequently more time consuming than the usual LKKR schemes,[5,6] but does provide a completely general way of balancing the two basis sets used. The technique has been applied to a Σ5 tilt grain boundary in nickel, with very satisfactory results, giving solutions which converge with 15 and 18 partial waves, nine for each of the nickel atom in each layer.

ACKNOWLEDGMENTS

J.M.M. acknowledges support from the U.S. Department of Energy and S.C. from the U.K. Science and Engineering Research Council. D.D.V. and S.C. gratefully acknowledge support from The Office of Naval Research, NATO, and the hospitality of Los Alamos National Laboratory, where this work was undertaken.

[1]J. B. Pendry, *Low-Energy Electron Diffraction* (Academic, London, 1974).
[2]A. P. Chen, Phys. Rev. B **3**, 4200 (1972).
[3]D. W. Jepsen, P. M. Marcus, and F. Jona, Phys. Rev. B **5**, 3933 (1972).
[4]K. Kambe, Surf. Sci. **117**, 443 (1982).
[5]J. M. Maclaren, S. Crampin, D. D. Vvedensky, and M. E. Eberhart, Phys. Rev. Lett. **63**, 2586 (1989); S. Crampin, D. D. Vvedensky, J. M. MacLaren, and M. E. Eberhart, Mater. Res. Soc. Symp. Proc. **141**, 373 (1989).
[6]C. Noguerra, D. Spanjaard, and D. W. Jepsen, Phys. Rev. B **17**, 607 (1978); G. Wachutka, *ibid.* **36**, 4725 (1987); F. Màca and M. Scheffler, Comput. Phys. Commun. **38**, 403 (1985).
[7]See, for example, p. 128 of Ref. 1.
[8]J. M. MacLaren, S. Crampin, D. D. Vvedensky, and J. B. Pendry, this issue, the preceding paper, Phys. Rev. B **40**, 12 164 (1989).
[9]J. F. L. Hopkinson, J. B. Pendry, and D. J. Titterington, Comput. Phys. Commun. **19**, 69 (1980); J. B. Pendry, Surf. Sci. **57**, 679 (1976).
[10]J.-H. Xu, T. Oguchi, and A. J. Freeman, Phys. Rev. B **36**, 4186 (1987); Mater. Res. Soc. Symp. Proc. **133**, 75 (1989).
[11]S. P. Chen, A. F. Voter, and D. J. Srolovitz, Scr. Metall. **20**, 1389 (1986); S. P. Chen, D. J. Srolovitz, and A. F. Voter, J. Mater. Res. **4**, 62 (1989).
[12]N. A. W. Holzwarth and M. J. G. Lee, Phys. Rev. B **18**, 5350 (1978).
[13]M. A. Van Hove and S. Y. Tong, *Surface Crystallography by LEED* (Springer-Verlag, Berlin, 1979).
[14]A. Gonis, Phys. Rev. B **34**, 8313 (1986).
[15]X.-G. Zhang and A. Gonis, Phys. Rev. Lett. **62**, 1161 (1989).
[16]K. Kambe, Z. Naturforsch. **22a**, 322 (1967); **22a**, 422 (1967); **23a**, 1280 (1968).
[17]See, for example, p. 138 of Ref. 1.
[18]V. L. Moruzzi, J. F. Janak, and A. R. Williams, *Calculated Electronic Properties of Metals* (Pergamon, New York, 1978).
[19]S. Crampin, D. D. Vvedensky, J. M. MacLaren, and M. E. Eberhart, Phys. Rev. B **40**, 3413 (1989).